First simultaneous observations of daytime MSTIDs over North America using GPS-TEC and DEMETER satellite data

Tatsuo Onishi, Takuya Tsugawa, Yuichi Otsuka, Jean-Jacques Berthelier, Jean-Pierre Lebreton

First simultaneous observations of daytime MSTIDs over North America using GPS-TEC and DEMETER satellite data

Tatsuo Onishi,[1] Takuya Tsugawa,[2] Yuichi Otsuka,[3] Jean-Jacques Berthelier,[1] and Jean-Pierre Lebreton[4]

Received 12 March 2009; revised 25 April 2009; accepted 7 May 2009; published 5 June 2009.

[1] We present simultaneous observations of daytime medium-scale traveling ionospheric disturbances (MSTIDs) over North America, using measurements of the Total Electron Content (TEC) by the US GPS network and ionospheric plasma data from the DEMETER micro-satellite. Several events show latitudinal variations of the plasma parameters at satellite altitude corresponding to the MSTID structures revealed on 2D TEC maps. In a case study with a very well defined MSTID, quasi periodic variations of the plasma density and of the ion velocity parallel to the Earth's magnetic field are observed along the satellite orbit that match the signature of the MSTID on the TEC maps. We believe it is the first simultaneous observation of parallel plasma motion in the topside ionosphere and propagating MSTID structures in the F-region. An initial analysis of this event is performed in the light of results from simple model of ionospheric disturbances associated with Atmospheric Gravity Waves (AGWs).
Citation: Onishi, T., T. Tsugawa, Y. Otsuka, J.-J. Berthelier, and J.-P. Lebreton (2009), First simultaneous observations of daytime MSTIDs over North America using GPS-TEC and DEMETER satellite data, *Geophys. Res. Lett.*, *36*, L11808, doi:10.1029/2009GL038156.

1. Introduction

[2] Medium-scale traveling ionospheric disturbances (MSTIDs) are quasi-periodic ionospheric plasma perturbations with typical horizontal wavelengths of several hundreds km and periods between 15 and 60 minutes. Daytime MSTIDs are produced by atmospheric gravity waves (AGWs) that are most often generated at high latitude and propagate towards the equator (see reviews by *Hunsucker* [1982] and *Hocke and Schlegel* [1996]). Following the pioneering work of *Hines* [1960], many theoretical, observational and model studies have been conducted over the last 30 years to understand the complex chain of physical processes that take place during the development and propagation of MSTIDs.

[3] Large Scale TIDs (LSTIDs) associated with strong magnetic activity move at large speeds of several hundreds m/s with long wavelengths (>1000 km) and periodicity (0.5 ~ 3.0 hours). The intensified auroral electrojets dissipate large amounts of energy in the lower thermosphere, giving rise to large scale AGWs that propagate away from the auroral zone. The AGW structure is then imparted to the ionospheric plasma, generating LSTIDs.

[4] Since the mid 1990s, high resolution two-dimensional Total Electron Content (TEC) maps have been made available over Japan and North America, where dense GPS networks are installed and provide continuous data [e.g., *Tsugawa et al.*, 2007, and references therein]. These maps constitute a unique tool to reveal the detailed features of the spatial structure and evolution of MSTIDs.

[5] There are very few in-situ satellite observations of MSTIDs in the ionosphere. Using data from Dynamics Explorer 2 satellite, *Johnson et al.* [1995] reported quasi-sinusoidal patterns of vertical velocity of both ions and neutrals over the polar caps. *Shiokawa et al.* [2003] discussed a simultaneous ground-satellite observation of a nighttime MSTID event using DMSP F15 satellite data and airglow images from ground-based observation. From the DEMETER initial satellite data, quasi-periodic variations of plasma parameters were also observed at sub-auroral latitudes. It was suggested that these variations were associated with AGW/TID [*Berthelier et al.*, 2006]. The present paper deals with the first simultaneous observations of daytime MSTID using GPS-TEC and DEMETER plasma parameters over North America.

[6] In the first section the GPS-TEC and DEMETER plasma data are briefly described, then, in the second section we present a few events for which a comparison between the two sets of data was possible. In conclusion, we briefly discuss the results obtained for one of these events in the frame of a simple model of the propagation of the MSTIDs in the F-region.

2. Description of Measurements

[7] The TEC data obtained from the GPS receiver network in North America have been selected for this study because they offer a dense coverage over a wide area, allowing at least one comparison with satellite data per day. As of January 2008, more than 1700 receivers are available, each of which calculates and records the slant TEC values every 30 seconds from 5 ~ 8 visible GPS satellites with elevation angle larger than 30 degrees. In the TEC map construction, we have employed the same method as that of *Tsugawa et al.* [2007] as follows. Integer cycle ambiguities and instrumental biases contained in each receiver-satellite data set are removed by detrending the data with a 60-minute running average, which is longer than a typical MSTID periodicity (10 ~ 60 minutes) [*Hunsucker*,

[1]LATMOS, IPSL, CNRS, St-Maur-des-Fossés, France.
[2]National Institute of Information and Communications Technology, Koganei, Japan.
[3]Solar-Terrestrial Environment Laboratory, Nagoya University, Nagoya, Japan.
[4]RSSD, ESTEC, ESA, Noordwijk, Netherlands.

0094-8276/09/2009GL038156

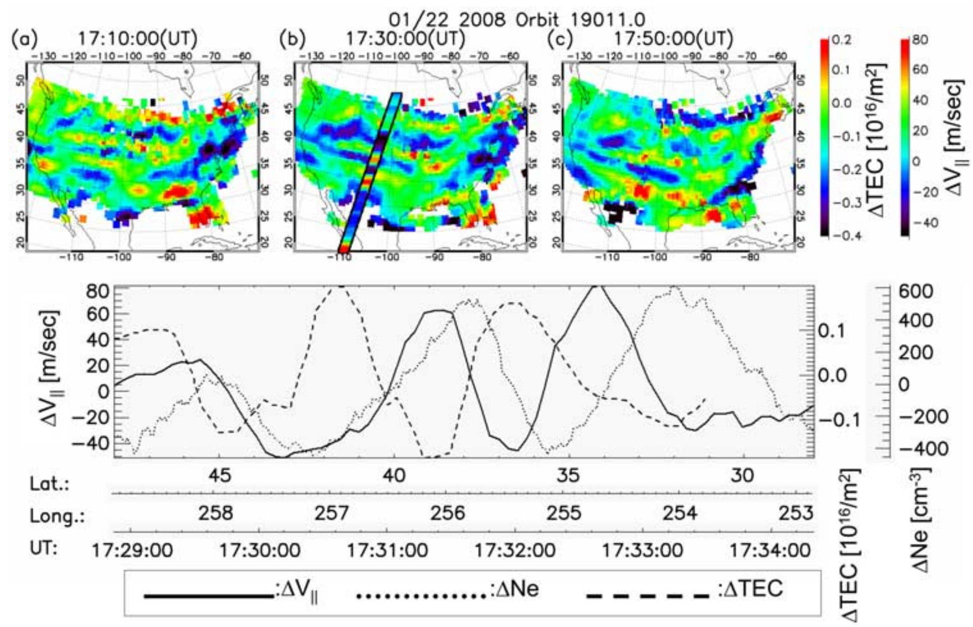

Figure 1. (top) GPS-TEC map over the US region on Jan. 22nd, 2008, with the $\Delta V_{\parallel}$ variation along DEMETER sub-orbit 19011.0 and (bottom) IAP $\Delta V_{\parallel}$, ΔTEC and ISL ΔNe along the satellite's orbit.

1982]. The vertical TEC value, or simply the TEC value, is then obtained by multiplying the slant TEC by a factor defined by the ratio of the "ionospheric thickness" taken equal to 200 km to the line-of-sight (LOS) length. The position assigned to every TEC measurement is defined by the point on the LOS at an altitude of 300 km. These simplifying assumptions are usually made in TEC studies since the F-region of the ionosphere, which provides the main contribution to the TEC, peaks at an average altitude of 300 km and has a typical thickness of about 200 km (for more details on TEC determination see, e.g., *Mannucci et al.* [1999]). The resulting values are then binned and averaged in pixels of 0.5° × 0.5° resolution in latitude and longitude. The map of the detrended TEC, ΔTEC, is then constructed with a spatial resolution of 1.5° × 1.5° by smoothing over 3 × 3 pixels and with a temporal resolution of 10 minutes, by averaging over 20 30-sec time frames. Examples of ΔTEC maps are shown in Figure 1 (top).

[8] DEMETER is the first micro-satellite in the CNES MYRIAD program, currently orbiting on a nearly circular sun-synchronous orbit at 650 km altitude with a descending node at ~10:30 LT on the day-time part of the orbits. The IAP (for Instrument Analyseur Plasma) Plasma Analyzer makes use of two analyzers: APR (for Analyseur à Potentiel Retardateur) performs the energy analysis of the rammed ionospheric ions and ADV (for Analyseur de Direction de Vitesse) determines the direction of arrival of the rammed ions [*Berthelier et al.*, 2006]. We use the ion velocity data from APR and ADV to compute the component of the ion velocity parallel to the Earth's magnetic field (referred to hereafter as the parallel ion velocity) which is counted positive for an upward ion motion. Electron density data from the ISL (for Instrument Sonde Langmuir) Langmuir probe [*Lebreton et al.*, 2006] have been used in the case study discussed in the last section. As explained in more detail below, satellite data are similarly detrended and averaged to filter out quasi DC shifts and fast fluctuations due to the small scale ionospheric irregularities and/or instrument noise.

3. Observations

[9] Figure 1 (top) shows three GPS ΔTEC maps obtained during a time interval of 40 minutes, from 17:10:00 UT to 17:50:00 UT with a time-step of 20 minutes. This interval of time encompasses the DEMETER pass over the central region of the USA on January 22, 2008 in the day-time part of orbit 19011 (referred to hereafter as sub-orbit 19011.0). On the map in Figure 1b, the variations of the parallel ion velocity are displayed colour coded along the orbit track. From the bands of enhanced ΔTEC values seen on the maps, the distances between bands and their temporal evolution, an east-west elongated MSTID structure can be recognized. It extends between the western and the central regions of the USA (Long: −120° ~ −90° and Lat: 36°N ~ 44°N) with a wavelength of about 400 km and a southward (equatorward) propagation velocity of about 100 m/sec.

[10] Figure 1b at 17:30:00(UT) corresponds to the average time when the satellite flies over the region of interest. The satellite crosses the US northern boarder at 17:28:00 UT and leaves the region covered by the GPS network at ~17:36:00 UT, corresponding to a latitude interval from ~48°N to ~28°N. For the purpose of comparison with ΔTEC observations, the positions of measurements shown in Figure 1b are those of the satellite northern conjugate point at 300 km. This allows us to compare ΔTEC and in-situ plasma measurements on the same magnetic field line. The parallel ion velocity data are actually subject to small scale fluctuations. To reduce the fluctuation level, the data are smoothed over a length equivalent to 2 degrees of latitude and detrended with 10-degree running averages in latitude which provides the detrended values $\Delta V_{\parallel}$ of the parallel ion velocity. The overlapped images of $\Delta V_{\parallel}$, and ΔTEC show an excellent correspondence, with a phase difference

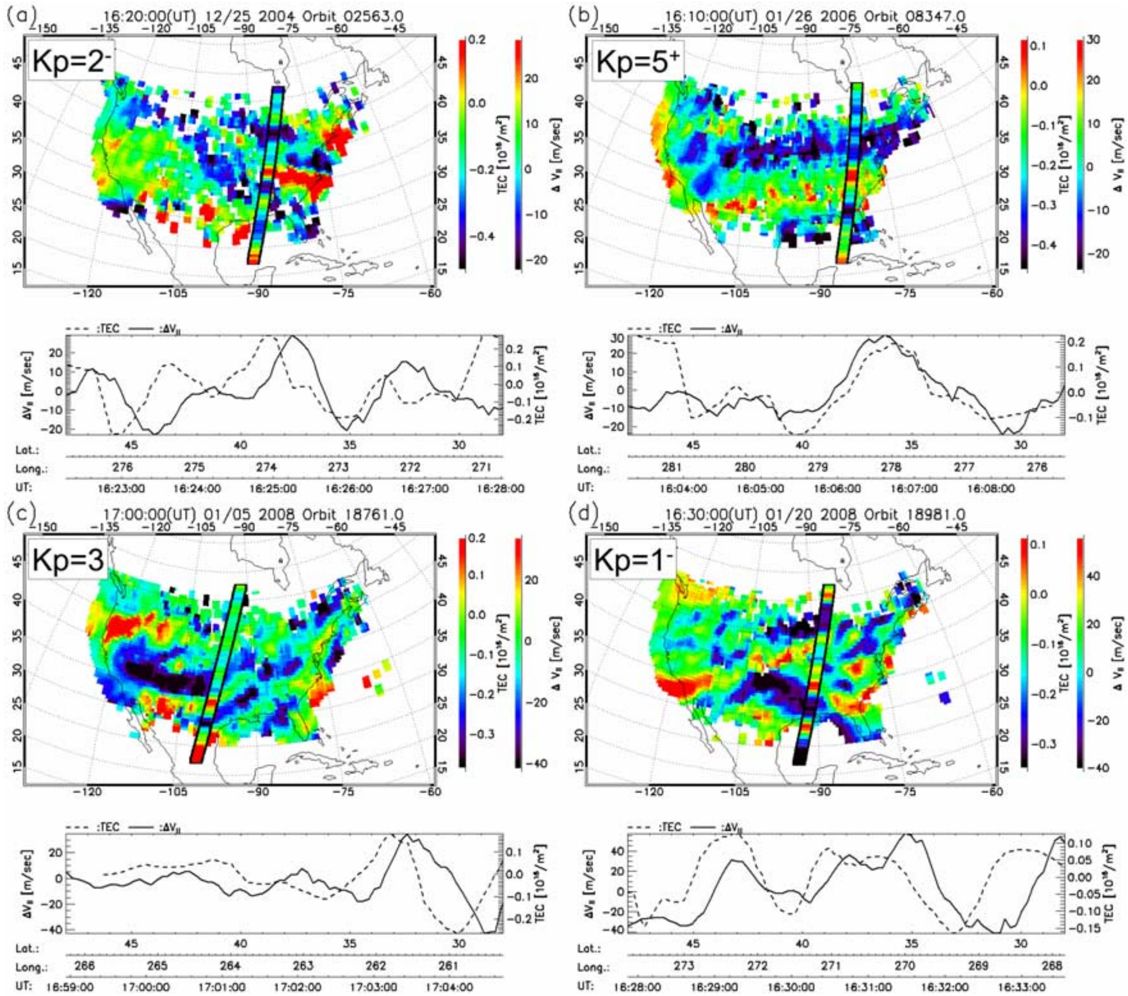

Figure 2. Various cases of TID observation by GPS-TEC and DEMETER IAP instrument. (a–c) Same type as in Figure 1 except for ISL electron density data is plotted. In Figure 2b, LSTID associated with a strong magnetic activity is shown with a negligible phase difference between ΔTEC and $\Delta V_{\|}$ due to its long wavelength. In the other cases, the phase difference of 1 $\sim$ 2 degrees is observed.

between the latitudinal profiles of the two parameters along the satellite orbit. Both $\Delta V_{\|}$, and ΔTEC display 3 peaks at 46°N, 39°N and 34°N and at 47°N, 42°N and 36.5°N, respectively.

[11] In Figure 2, several other cases of simultaneous observations of MSTID by the GPS network and DEMETER are presented. In Figures 2a–2d, the ΔTEC map at the moment indicated and the $\Delta V_{\|}$ variation along the orbit are shown as in Figure 1. All cases show a good correlation of $\Delta V_{\|}$ in the top-side ionosphere with the MSTID structures in the denser ionosphere close to the F-region peak.

[12] To allow for an easier quantitative comparison, curves of ΔTEC and $\Delta V_{\|}$ values have been plotted in Figure 1 (bottom) below the colour maps. In these plots the ΔTEC values have been calculated slightly differently by taking, for a given time and coordinates of the satellite, the 5-minute running average of ΔTEC values. Time and coordinates indicated in the horizontal axis are those from the satellite's orbit and the ΔTEC value at each point corresponds to the value at the satellite northern conjugate point at 300 km altitude. The $\Delta V_{\|}$ is shown by a solid line and ΔTEC values by a dashed line. Since we are interested in a relative correlation of the parameters, a spatial detrending with 10-degree running average in latitude is applied to ΔTEC as it is applied on $\Delta V_{\|}$.

[13] The satellite velocity (7.5 km/sec) is much faster than the MSTID propagation speed (100 m/sec). Therefore the satellite observations provide, at the time of the satellite pass, a nearly instantaneous snapshot of the ionosphere over the whole area where the MSTID structure is revealed by the ΔTEC geographical maps.

[14] When the angle between the satellite orbital velocity and the MSTID propagation direction normal to the wavefront is large, the apparent wavelength of the MSTID on satellite data can be larger than its actual value. Since the satellite orbital velocity in day-time sub-orbit is inclined $\sim$8° towards the west, the wavelength of an MSTID with a wave front inclined from south-west to north-east, thus propagating south-eastward would appear larger and this effect has to be corrected. Among the various cases that have been studied, the $\Delta V_{\|}$ variations range from 5 to 50 m/sec per 0.1 TECU of ΔTEC. From the comparison of several MSTID events (not shown here), we have noted that the amplitude of $\Delta V_{\|}$ becomes smaller, when the MSTID

propagates at a larger angle with respect to the geomagnetic plane. In such cases, the AGW component of the neutral gas velocity along the Earth's magnetic field is smaller. Since the component of the neutral velocity along the Earth's magnetic field is transferred to the ions through neutral-ion collisions, the resulting parallel ion velocity is likewise smaller in accordance with observations.

[15] ΔTEC and $\Delta V_{||}$ from Orbit 19011.0 are shown in Figure 1 (bottom) together with the satellite measurement of the detrended electron density variations ΔNe (dotted line). To get the ΔNe variations, the electron density data are processed similarly as the parallel ion velocity data with a 10-degree detrending and 2-degree smoothing. In most of the events analyzed thus far, the electron density data display quite large fluctuations which often mask the presence of well defined regular variations but sub-orbit 19011.0 is one case in which ΔNe shows clear periodic variations that are in very good agreement with those of ΔTEC and $\Delta V_{||}$. The MSTID structure is recognized between 30°N and 45°N on all parameters. The local maxima of $\Delta V_{||}$ at 46°N, 39°N and 34°N latitudes correspond to three maxima of ΔTEC at 47°N, 42°N and 36.5°N latitudes, respectively. Three maxima of ΔNe can also be recognized at 45°N, 38°N and 32°N latitudes, corresponding to the three maxima of two other parameters.

[16] The observations displayed in Figure 1 (bottom) can be summarized as follows.

[17] 1. ΔTEC and ΔNe. With the above mentioned simplifying assumptions on TEC measurements, ΔTEC and ΔNe represent the electron density variations at two different altitudes, the peak of the F-layer near 300 km and the satellite altitude at 650 km. (a) The maxima in ΔNe are shifted toward the equator with respect to the maxima in ΔTEC. (b) The latitude shift becomes larger at lower latitude: the shift in latitude between two peaks is $\sim$3° for the ΔTEC maximum at $\sim$42° while it increases to $\sim$5° at lower latitude (ΔNe peak at 32°N and ΔTEC peak at 37°N).

[18] 2. $\Delta V_{||}$ and ΔNe. (a) Peaks in $\Delta V_{||}$ (namely at 34°N, 39°N and 45.5°N) are always found on a slope of the ΔNe that increases from a trough to a peak (at 32°N, 38°N and 45°N, respectively) toward the equator, implying that the phase difference is in the range from 0° to 180°. (b) The phase difference also becomes larger at lower latitudes.

4. Discussion and Conclusion

[19] Since the ion density in the upper F-region is much smaller than the neutral density, the ion motion has little feedback on the neutral motion and the ionospheric ions may be considered as a passive tracer of the neutral gas disturbances. The ions are magnetized and, in presence of an AGW, can only move along the magnetic field lines with a velocity equal to the component of the neutral gas velocity parallel to the Earth's magnetic field. *Hooke* [1968] has analyzed the temporal and spatial variations of the plasma density and ion velocity in TIDs in the altitude range where ion and neutrals are effectively coupled by collisions. For a neutral density $n_N \sim 10^{15} m^{-3}$, an ion density $n_i \sim 10^{11} m^{-3}$ and temperature $T \sim 1000$ K at the peak of the F-layer near 300 km, the ion-neutral collision frequency is $\sim$1.0 Hz. This number reduces to 10^{-4} Hz at the satellite altitude, thus much smaller than the AGW frequency. The collisional/non-collisional boundary is therefore between 300 km and the satellite altitude, at about 450 km altitude as shown by *Hooke* [1968]. *Hooke* [1968] used a plane wave approximation for the AGW and a simple model based on the continuity equation for the ionospheric plasma. His results show that, in this altitude range, the disturbances of the plasma density ΔNe are organized along phase fronts that reproduce the propagating phase fronts of the neutral gas density and move at the same velocity as the AGW. The variations of $\Delta V_{||}$ are organized along a similar pattern with moving phase fronts and there is a phase difference, $\Delta\Phi$, which was derived by *Hooke* [1968] as a function of two parameters of the AGW propagation vector, the component along the magnetic field and the vertical damping rate, as well as of the local scale height of the undisturbed plasma. Thus the phase difference, $\Delta\Phi$, between the plasma velocity and density disturbances varies with altitude.

[20] At altitude above $\sim$450 km in the top-side ionosphere, neutral-ions collisions become negligible and the dynamics of the ionospheric plasma is controlled by its transport along magnetic field lines. To describe the propagation of the plasma disturbances we may refer to the work of *Marchand and Berthelier* [2008]. Using the two-dimensional ionospheric model SAMI2, these authors have studied the ionospheric disturbances following an earthquake and associated with the acoustic pulse which is generated by the main shock and propagate in the neutral atmosphere above the epicenter region. Their results show that, in the top-side ionosphere up to the DEMETER altitude, thus above our collisional boundary, plasma disturbances propagate along the magnetic field at the ion acoustic velocity, of the order of 1 to 2 km/s, without significant variation in the phase difference between the plasma density and parallel velocity disturbances. The distance that the MSTID travels at 100 m/sec, while an ion acoustic wave travel up to the DEMETER's altitude, is a few tens of kilometers and is therefore negligible with respect to the size of the MSTID structure at 300 km altitude. We can thus neglect in practice the propagation delay in the non-collisional altitude when comparing the DEMETER plasma observations and the TEC data.

[21] In Figure 3, we have given a schematic interpretation of our observations by assuming for simplicity an AGW and its associated MSTID propagating in a geomagnetic plane and considering two separate regions in the upper atmosphere separated by the collisional/non-collisional boundary at $\sim$450 km. The variations of the neutral gas density have been represented by a grey-scale contour with the dense grey depicting the position of the maximum density. At high altitudes, in the tenuous non collisional upper atmosphere, the AGW become evanescent and, due to the higher atmospheric viscosity [*Pitteway and Hines*, 1965], the neutral density structures are organized along the vertical direction. At lower altitudes the velocity of the neutral gas, represented by arrows in Figure 3, oscillates in the direction parallel to the phase front of the AGW. In the collisional regime studied by Hooke, $\Delta V_{||}$ variations coincide with the AGW variations of the neutral gas velocity. The ΔNe variations are organized along a similar phase front structure with a phase difference $\Delta\Phi$ between the ΔNe and the $\Delta V_{||}$ maxima as shown in Figure 3 where $\Delta\Phi$ has been chosen in

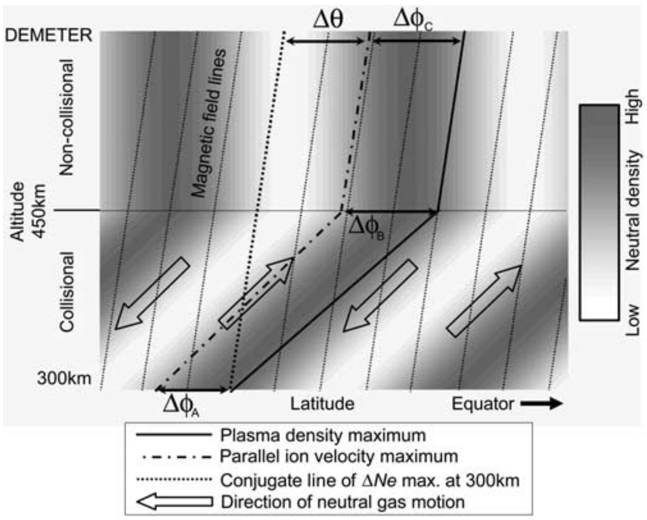

Figure 3. Schematic representation of the AGW/MSTID induced structures of the variations of the neutral gas and plasma density and velocity. The phase difference, $\Delta\Phi$, between $\Delta V_{\|}$ and ΔNe is variable in the collisional regime ($\Delta\Phi_A \neq \Delta\Phi_B$), whereas in the non-collisional regime, it is constant ($\Delta\Phi_B = \Delta\Phi_C$). The observed relative phasing between ΔTEC and $\Delta V_{\|}$ is indicated by $\Delta\theta$.

accordance with the DEMETER observations in sub-orbit 19011.0. According to *Hooke* [1968], $\Delta\Phi$ varies with altitude, thus giving rise to $\Delta\Phi_A \neq \Delta\Phi_B$ in Figure 3. In the collisional zone, when one follows the equatorward propagating MSTID/AGW, the $\Delta V_{\|}$ maximum lags behind the ΔNe maximum and thus occurs at higher latitude. Above the collisional boundary ΔNe and $\Delta V_{\|}$ map along the magnetic field lines until the altitude of DEMETER with, according to the abovementioned article, negligible change in phase difference, i.e. $\Delta\Phi_B \approx \Delta\Phi_C$. Since DEMETER flies towards the equator, it observes the $\Delta V_{\|}$ maximum prior to the ΔNe maximum i.e. at higher latitude. Due to the respective inclination of the AGW phase front and magnetic field lines, DEMETER encounters the magnetic field line on which the ΔTEC maximum (assumed to correspond to the ΔNe maximum at 300 km) at a higher latitude than both the ΔNe and $\Delta V_{\|}$ maxima. Some cases actually occur when the phase difference between ΔTEC maximum and $\Delta V_{\|}$ maximum, $\Delta\theta$, is observed to be small and even negligible as in Figure 2b which appears to correspond to an LSTID with a much larger wavelength than the MSTID shown in Figure 1. A simplified interpretative drawing (not shown here) similar to Figure 3 with a longer wavelength AGW shows that the larger $\Delta\Phi$ results in a shift of the ΔTEC maxima close to $\Delta V_{\|}$ maxima. In this letter, we focus on TIDs with moderate wavelengths that can be readily identified on the US TEC map. Further studies on LSTIDs may even show cases with negative $\Delta\theta$.

[22] As shown in Figure 1 the phase differences between the maxima of the three parameters ΔTEC, ΔNe and $\Delta V_{\|}$ increase along the path of the MSTID towards the equator. We believe that this is a phenomenon observed for the first time and may give a fruitful information on the AGW propagation mechanism over a long latitudinal range. A detailed discussion of this effect is beyond the scope of this paper but a simple idea may be suggested based on an increasing inclination of the propagation vector with respect to the horizontal along the path of the AGW. This would induce simultaneously a larger phase difference between the maximum of ΔTEC and ΔNe and between the maxima of ΔNe and $\Delta V_{\|}$. However the reality is certainly much more complex and the detailed understanding of the observations will require a more thorough analysis and modeling effort currently in progress.

[23] **Acknowledgments.** The GPS data used in this study were obtained via the ftp servers of CORS (ftp://www.ngs.noaa.gov/cors/rinex/), SOPAC (ftp://garner.ucsd.edu/pub/rinex/), and IGS (ftp://cddisa.gsfc.nasa.gov/pub/gps/data/daily/). We acknowledge the IGS, UNAVCO, SCIGN and its sponsors, the W.M. Keck Foundation, NASA, NSF, USGS, SCEC for providing GPS data. This work was supported by funding from CNES under grant CNES-EU60015. We thank F. Bertrand for his participation to the DEMETER data processing.

References

Berthelier, J.-J., M. Godefroy, F. Leblanc, E. Séran, D. Peschard, P. Gilbert, and J. Artru (2006), IAP, the thermal plasma analyzer on DEMETER, *Planet. Space Sci.*, *54*, 487–501.

Hines, C. O. (1960), Internal atmospheric gravity waves at ionospheric heights, *Can. J. Phys.*, *38*, 1441–1481.

Hocke, K., and K. Schlegel (1996), A review of atmospheric gravity waves and traveling ionospheric disturbances: 1982–1995, *Ann. Geophys.*, *14*, 917–940.

Hooke, W. H. (1968), Ionospheric irregularities produced by internal atmospheric gravity waves, *J. Atmos. Terr. Phys.*, *30*, 795–823.

Hunsucker, R. D. (1982), Atmospheric gravity waves generated in the high latitude ionosphere: A review, *Rev. Geophys.*, *20*, 293–315.

Johnson, F. S., W. B. Hanson, R. R. Hodges, W. R. Coley, G. R. Carignan, and N. W. Spencer (1995), Gravity waves near 300 km over the polar caps, *J. Geophys. Res.*, *100*, 23,993–24,002.

Lebreton, J. P., S. Stverak, P. Travnicek, M. Maksimovic, D. Klinge, S. Merikallio, D. Lagoutte, B. Poirier, Z. Kozacek, and M. Salaquarda (2006), The ISL Langmuir Probe experiment and its data processing onboard DEMETER: Scientific objectives, description and first results, *Planet. Space Sci.*, *54*, 472–486.

Mannucci, A. J., B. A. Iijima, U. J. Lindqwister, X. Pi, L. Sparks, and B. D. Wilson (1999), GPS and ionosphere, in *Review of Radio Science 1996-1999*, edited by W. R. Stone, pp. 625–665, Int. Union of Radio Sci., Ghent, Belgium.

Marchand, R., and J.-J. Berthelier (2008), Simple model for post seismic ionospheric disturbances above an earthquake epicentre and along connecting magnetic field lines, *Nat. Hazards Earth Syst. Sci.*, *8*, 1341–1347.

Pitteway, M. L. V., and C. O. Hines (1965), The reflection and ducting of atmospheric acoustic-gravity waves, *Can. J. Phys.*, *43*, 2222–2243.

Shiokawa, K., Y. Otsuka, C. Ihara, T. Ogawa, and F. J. Rich (2003), Ground and satellite observations of nighttime medium-scale traveling ionospheric disturbance at midlatitude, *J. Geophys. Res.*, *108*(A4), 1145, doi:10.1029/2002JA009639.

Tsugawa, T., Y. Otsuka, A. J. Coster, and A. Saito (2007), Medium-scale traveling ionospheric disturbances detected with dense and wide TEC maps over North America, *Geophys. Res. Lett.*, *34*, L22101, doi:10.1029/2007GL031663.

J.-J. Berthelier and T. Onishi, LATMOS, IPSL, CNRS, 4 avenue de Neptune, F-94107 St-Maur-des-Fossés CEDEX, France. (tatsuo.onishi@latmos.ipsl.fr)

J.-P. Lebreton, RSSD, ESTEC, ESA, Keplerplaan 1, NL-2200 AG Noordwijk, Netherlands.

Y. Otsuka, Solar-Terrestrial Environment Laboratory, Nagoya University, Furo-cho, Chikusa-ku, Nagoya 464-8601, Japan.

T. Tsugawa, National Institute of Information and Communications Technology, 4-2-1 Nukui-Kitamachi, Koganei, Tokyo 184-8795, Japan.